Hindawi
Shock and Vibration
Volume 2019, Article ID 2592459, 16 pages
https://doi.org/10.1155/2019/2592459

Research Article

SHPB Test and Microstructure Analysis on Ready-Mixed Concrete in Uniaxial Load and Passive Confining Pressure States

Jing-shuang Zhang[1,2], **Xue-lei Duan**[1,2] **and Zi-yan Yang**[1,2]

[1]*Engineering Research Center of Underground Mine Construction, Ministry of Education, Anhui University of Science and Technology, Huainan, Anhui 232001, China*
[2]*School of Civil Engineering and Architecture, Anhui University of Science and Technology, Huainan, Anhui 232001, China*

Correspondence should be addressed to Xue-lei Duan; dxlaust@163.com

Received 17 June 2019; Revised 11 August 2019; Accepted 22 August 2019; Published 23 September 2019

Academic Editor: Marco Alfano

Ready-mixed concrete has been used as a support in mine roadways, where the impact load of blasting excavation can cause damage to the concrete support of the roadway. However, limited studies are available on the effect of water content, storage period, and impact pressure on dynamic mechanical properties of ready-mixed concrete in uniaxial load and passive confining pressure states. To investigate the effect of water contents (0%, 1.0%, 1.5%, and 2.0% by mass of dry sand), storage periods (0 d, 3 d, 7 d, 15 d, 20 d, and 30 d), and impact pressures (0.6 MPa and 0.9 MPa) on dynamic mechanical properties of ready-mixed concrete in uniaxial load and passive confining pressure states, the dynamic compression test using split Hopkinson pressure bar (SHPB) has been carried out. In addition, the microscopic test based on the scanning electron microscope (SEM) is conducted to analyze the effect of water content and storage period on the microstructure of ready-mixed concrete. The experimental results show that under the conditions of uniaxial load and passive confining pressure, the dynamic compressive strength of ready-mixed concrete decreases with the increase of water content and storage period but increases with the increase of impact pressure. At the same impact pressure, the dynamic compressive strength in passive confining pressure state is larger than that in uniaxial load state. The dynamic stress-strain curves of ready-mixed concrete in uniaxial load and passive confining pressure states can be divided into three stages: elastic stage, plastic stage, and failure stage. The peak strain increases with increasing impact pressure, and the peak strain in passive confining pressure state is more than that in uniaxial load state. The degree of damage for ready-mixed concrete specimens increases with the increase of the storage period and water content; however, the damage of specimens in passive confining pressure state is less than that of specimens in uniaxial load state. Meanwhile, an analysis to the microstructural mechanism of water content and storage period inside of ready-mixed concrete has been performed.

1. Introduction

Concrete is an important building material that is used in complex construction conditions such as platforms, nuclear power plants, mines, tunnels, and wellbore protective layers [1–3]. Research data indicate that more than 95% of Chinese coal mines are mined by underground well mining [4, 5]. Mine roadway plays an important role in providing underground engineering for ventilation, production, transportation, and blanking, using concrete structures for supporting the mine and the tunnel wall to ensure the safety of the mine [6, 7]. At present, the construction method adopted by most mines is onsite artificial mixing in the mine construction area, which results in the following problems [8, 9]: (1) The space on the construction site becomes more crowded, reducing work efficiency and affecting construction progress. (2) Inaccurate measurement of raw materials leads to inaccurate concrete mix which has a great impact on concrete performance, resulting in waste of raw materials and increasing cost. (3) The dust concentration of mine roadway increases, which seriously affects the mine environment and causes damage to the physical and mental health of the staff.

To solve the above problems in the actual engineering of the mine, according to the requirements of green construction, ready-mixed concrete that is a new material used for mine roadway and inner wall support is proposed [10]. According to the ready-mixed concrete (GB/T 14902-2012) [11], concrete produced at the mixing station and delivered to construction site by means of transport equipment is defined as ready-mixed concrete, which has the following advantages: (1) high construction efficiency, reduced construction period, and cost savings; (2) centralized configuration, ensuring accurate mix ratio, and improving project quality; (3) application convenience, green health, and environmental protection. Therefore, the static mechanical and physical properties of ready-mixed concrete have been investigated by many scholars. Alhozaimy [12] studied the effect of retempering on the compressive strength of ready-mixed concrete in hot-dry environments and found that due to water addition, the reduction in compressive strength was proportional to the associated increase in slump, which could use the change in slump to predict reduction of strength in the case of jobsite water additions. Gebremichael et al. [13] added ready-mixed concrete into returned fresh concrete (RFC) and obtained that mixing RFC with ready-mixed concrete was a suitable alternative for recycling RFC, which meant higher economic value and environmental benefits. Zhang and Ma [14] studied the influence of water content and expansion agent on the microstructure of the ready-mixed shrinkage concrete and pointed out that the inclusion of 6% expansion agent could excellently improve its internal compactness, while the increase of water content led to the increase of porosity and the decrease of compactness. Basar and Deveci Aksoy [15] investigated the effect of waste foundry sand (WFS) on mechanical and microstructural properties of ready-mixed concrete, indicating that the addition of WFS as partial replacement of sand increased the water absorption ratio of the concrete mixtures and also reduced the strength and density of ready-mixed concrete. Zhang and Ma [16] studied the effect of different water contents and storage periods on static compressive strength of ready-mixed concrete, which obtained that the static compressive strength of ready-mixed concrete decreased with increasing storage period and water content; meanwhile, the mechanism of this phenomenon was explained.

However, concrete structures are not only subjected to static loads but also subjected to dynamic loads such as mining vibrations, rock blasting in the support of mine roadways, and underground engineering [17–20]. The blasting excavation impact load of the artillery mines will cause the instability of the roadway. According to statistics, more than 50% of artillery mines in China have the dynamic instability problems of roadway, which are mainly due to impact pressure and gas leakage [21, 22]. The support structure of the mine roadway produces passive support reaction force on the wall of the ready-mixed concrete, which can be affected by various possible powers during the support. It is very important for the safety of the roadway to withstand this part of the power by the support structure of ready-mixed concrete. Due to the rate sensitivity, the dynamic mechanical properties of concrete are different from its static loads [23–26]. Jiao et al. [25] used fractal theory to establish dynamic damage constitutive relation of high-strength concrete and obtained the theoretical and experimental curves of test with good relationship. Kim et al. [26] studied the effect of maximum coarse aggregate size on dynamic compressive strength of high-strength concrete, which found that the larger maximum coarse aggregate sizes resulted in larger heterogeneity of specimens. Ma et al. [27] analyzed the dynamic mechanical properties of coral concrete with different strain rates, observing more remarkable rate dependence in dynamic compressive strength of coral concrete than other cement-based composites. Li et al. [28] studied the dynamic mechanical characteristics of filling layer self-compacting concrete under impact loading, which obtained that the dynamic strength increased with the increase of strain rate.

However, the theoretical and experimental study achievements of predecessors on mechanical behavior of ready-mixed concrete cited above are primarily concentrated on static mechanical properties (static compressive strength, static tensile strength, and static flexural strength) and dynamic strength of concrete. Limited studies are available on the dynamic mechanics of ready-mixed concrete in uniaxial load and passive confining pressure states. The primary objective of this paper is to investigate effects of different water contents (0%, 1.0%, 1.5%, and 2.0% by mass of dry sand), storage periods (0 d, 3 d, 7 d, 15 d, 20 d, and 30 d), and impact pressures (0.6 MPa and 0.9 MPa) on the dynamic mechanics of ready-mixed concrete in uniaxial load and passive confining pressure states. The dynamic impact compression test based on the variable section split Hopkinson pressure bar with a diameter of 74 mm and the 45# steel sleeve used in passive confining pressure states is carried out. The dynamic compressive strength, dynamic stress-strain curves, dynamic elastic modulus, and failure modes are obtained in terms of water content, storage period, and impact pressure. Moreover, the microscopic mechanism of the water content and storage period on the dynamic properties of the ready-mixed concrete is analyzed using scanning electron microscope (SEM) analysis, and the test data are provided for the ready-mixed concrete in the underground engineering support.

2. Experimental Program

2.1. Materials and Mix Proportions. Ordinary Portland cement (P.O. 42.5) is selected for the concrete mixtures in the test. Its stability is qualified, and the fineness is 2%. After testing, the compressive strengths at 3 d and 28 d are 22.7 MPa and 59.2 MPa, respectively. Crushed stone is used as the coarse aggregate with 10~15 mm in particle sizes, and fine aggregate uses natural sands whose fineness modulus is 2.98, which is obtained from the shore of Huai River. The water from Huainan tap water is used for specimen preparation, which is in conformity with standards of water for concrete (JGJ 63-2006) [29]. The weight method is used for the proportion design of the mixture in the study. The ratio of water-cement-sand-stone is 0.45 : 1.00 : 2.07 : 2.07 by weight. In order to

investigate the effects of the water content and storage period on dynamic mechanical properties and failure mode of ready-mixed concrete, four percentages of water contents and six storage periods are adopted in this experiment.

2.2. Sample Preparation. All specimens are prepared to the experimental procedures described as follows: (1) The natural sand and stones are placed in an electric blast drying oven set at a temperature of 105°C for more than 12 h to a constant weight, which is cooled and sealed for storage to prevent absorption of moisture from the air during cooling. (2) Water used in the experiment is 0%, 1.0%, 1.5%, and 2.0% by weight of dry sand, which is added to the dry sand, then sealed and stored in an airtight container for 48 hours to ensure uniform dispersion of water in the sand. (3) According to the above design mix ratio, the prepared cement flour, dry stone, and sand with different water contents are put into mixer and water is added and stirred to make a ready-mixed dry material. The prepared ready-mixed dry material is sealed for storage. In order to prevent damage to the sealed bag during handling, the storage method uses the inner high-pressure flat pocket as a sealed bag and the outer snake-skin bag is stored as a load-bearing bag. Considering the actual demand of ready-mixed dry material during the construction, the storage period of ready-mixed dry material in the test is selected for 0 d, 3 d, 7 d, 15 d, 20 d, and 30 d.

After the corresponding storage period is reached, according to the standard for test method of mechanical properties on ordinary concrete (GB/T 50081-2002) [30], the concrete is made by using a self-made concrete mould. The finished concrete samples are placed into a standard moisture room with temperature maintained at (20 ± 2)°C and relative moisture above 95% for curing, and the curing duration is determined to be 28 d. Coring machine, cutting machine, and grinding machine are adopted to core, cut, and grind the specimen of ready-mixed concrete, which is processed into cylindrical shape with a height of 37 mm and a diameter of 74 mm, as shown in Figure 1. To reduce the effect of the processing differences on experimental results, specimens are carefully polished to ensure that surface planeness of the sample is controlled to ±0.005 mm and the vertical deviation of the upper and lower surface is ±0.25° [31]. Additionally, ultrasonic testing methods are adopted to preliminary screening test specimens, and samples with similar *P*-wave velocity are selected for the SHPB test by the two impact pressures (0.6 MPa and 0.9 MPa) in uniaxial load and passive confining pressure states. There are 48 groups of samples in the research, and eight sets of parallel specimens were prepared to control the accuracy of the result. For abbreviating, the samples are numbered by some symbols, and the meaning of abbreviation is in the following. The samples WC0-SP3-IP0.9-UL or WC0-SP3-IP0.9-PC are on behalf of the sample with 0% water content, 3 d storage period, and 0.9 MPa impact pressure in uniaxial load or passive confining pressure states.

2.3. SHPB Test

2.3.1. Apparatus and Experiment Procedure. SHPB equipment has been successfully used to investigate the dynamic

Figure 1: Ready-mixed concrete specimens.

behaviors of materials, such as rock [32, 33], concrete [34, 35], mortar [36], and frozen soil [37]. A split Hopkinson pressure bar with a diameter of 74 mm in the experiment is employed to investigate the dynamic mechanical behavior of ready-mixed concrete in uniaxial load and passive confining pressure states, as shown in Figure 2. The apparatus consists of the launching equipment, a striker bar, an incident bar, a transmitted bar, an absorbing bar, the buffer device, and a data acquisition unit, and the length of the striker bar, incident bar, and transmitted bar are 0.6 m, 2.4 m, and 1.2 m, respectively. These bars are made of high-strength alloy steel with Young's modulus of 210 GPa, the *P*-wave velocity of 5,190 m/s, and the density of 7800 kg/m^3. Two strain gauges are mounted on the incident and transmitted bars to record the origin strain signals, and the front of the incident bar adopts the pulse shaper, which is benefit to the stress equilibrium of the specimen [38, 39]. For the SHPB test of ready-mixed concrete in passive confining pressure state, the sleeve is made of 45# steel whose tensile strength is 600 MPa, the yield strength is 355 MPa, and the elastic modulus is 210 GPa, which is used as the hoop constraint for the specimen. The basic dimensions of the sleeve are shown in Figure 3.

The impact compressive test of ready-mixed concrete with different water contents and storage periods in uniaxial load and passive confining pressure states is tested by using two impact pressures of 0.6 MPa and 0.9 MPa. The detailed steps of uniaxial load and passive confining pressure measurement are as follows: (1) The semiconductor strain gauge is attached in the axial vertical direction of the steel sleeve to measure the radial dynamic response of the sample. (2) Appropriate lubricant is evenly smeared on the surface of the sample and the inner wall of the passive confining sleeve, which reduces the friction among the sample, the inner wall of the sleeve, and the contact surface of the bars. (3) The concrete specimens are put between the incident bar and the transmitted bar; meanwhile, the axis of the specimens, the incident bar, and the transmission bar are kept collinear. (4) Opening the gas pressure switch, striking the incident bar by striker bar, and collecting the fragment of the ready-mixed specimen are operated in sequence.

2.3.2. Data Processing. The SHPB test of ready-mixed concrete in uniaxial load and passive confining pressure states is based on the basic assumption of uniform stress and one-dimensional elastic stress wave theory, ignoring the inertial effect and friction effect of the sample [40]. As shown in Figure 4, the striker bar produce impacts on the incident

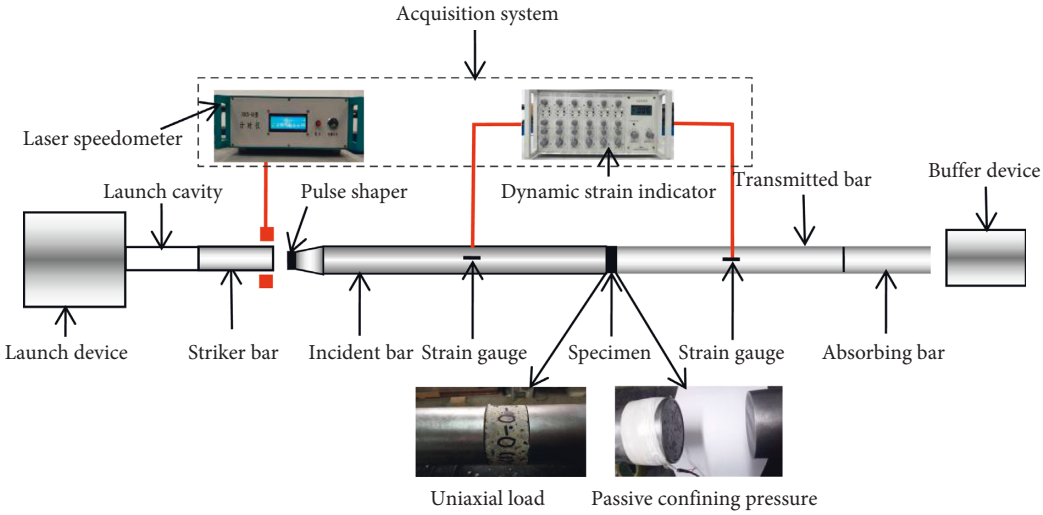

Figure 2: SHPB test apparatus of ready-mixed concrete specimens.

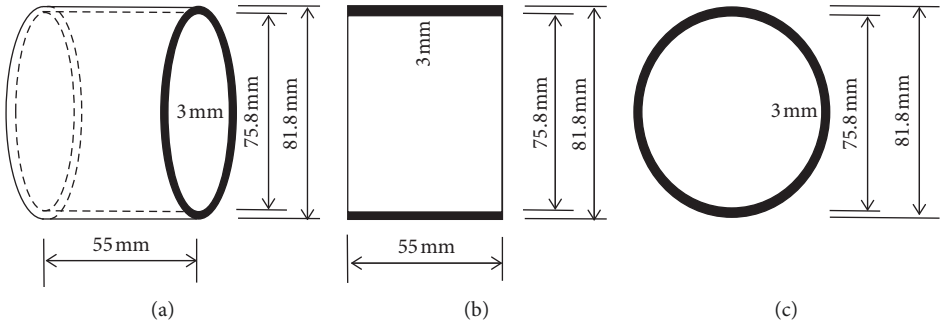

Figure 3: Basic dimensions of steel sleeve. (a) Stereogram. (b) Transverse profile. (c) Vertical profile.

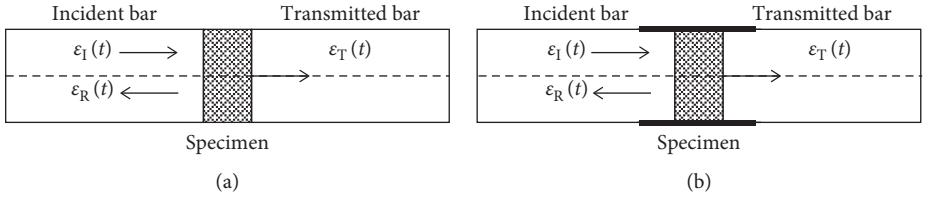

Figure 4: SHPB principle of ready-mixed concrete with different states. (a) Uniaxial load state. (b) Passive confining pressure state.

bar, and the incident stress pulse occurs and propagates along the incident bar to the interface of the incident bar and specimen, where part of the pulse causes the cylindrical sample to be radially deformed and the other generates a reflected pulse and a transmitted pulse due to the wave impedance of the incident bar and specimen.

According to the one-dimensional elastic wave theory, the wave velocity C_0 transmitted evenly along the rod is calculated by the following equation:

$$C_0 = \sqrt{\frac{E_0}{\rho_0}}, \tag{1}$$

where ρ_0 is the density of the bar material and E_0 is Young's modulus of the bar.

The stress $\sigma(t)$, strain $\varepsilon(t)$, and strain rate $\dot{\varepsilon}(t)$ in the concrete sample can be calculated according to the three wave methods [41]:

$$\begin{aligned}
\sigma(t) &= \frac{E_0 A_0}{2A_s}\left[\varepsilon_I(t) - \varepsilon_R(t) - \varepsilon_T(t)\right], \\
\varepsilon(t) &= \frac{C_0}{l_s}\int_0^\tau \left[\varepsilon_I(t) - \varepsilon_R(t) - \varepsilon_T(t)\right]dt, \\
\sigma(t) &= \frac{C_0}{l_s}\left[\varepsilon_I(t) - \varepsilon_R(t) - \varepsilon_T(t)\right],
\end{aligned} \tag{2}$$

where $\varepsilon_I(t)$, $\varepsilon_R(t)$, and $\varepsilon_T(t)$ are the strain of incident wave, reflected wave, and transmitted wave, respectively; A_0 and C_0 are the cross-sectional area and the elastic wave speed of the bar; A_s and l_s are the cross-sectional area and height of ready-mixed concrete specimen, respectively; t is the duration time of elastic wave.

The axial stress of ready-mixed concrete can be calculated by the three wave methods, and the passive confining

pressure applied by the sleeve to the ready-mixed concrete sample needs to be estimated by the circumferential waveform of the sleeve. The force state diagram of sleeve subjected to passive confining pressure is shown in Figure 5.

It is supposed that the passive confining pressure q is distributed on the inner wall of the sleeve whose inner and outer diameters are $2a$ and $2b$. The sleeve is always in an elastic state, and the force of sleeve ignores the displacement of the rigid body during the test. Based on the theory of elastic thick-walled cylinder [42], the radial normal stress and the hoop normal stress of the sleeve at each point can be calculated through the following equations:

$$\sigma_\rho = \frac{a^2 q}{b^2 - a^2}\left(1 - \frac{b^2}{\rho^2}\right), \tag{3}$$

$$\sigma_\varphi = \frac{a^2 q}{b^2 - a^2}\left(1 + \frac{b^2}{\rho^2}\right), \tag{4}$$

where ρ is the polar point of the force point inside the sleeve.

As can be seen from equation (4), the tensile stress on the inner wall ($\rho = a$) of the sleeve is the largest and the tensile stress on the outer wall ($\rho = b$) of the sleeve is the smallest, which can be calculated through the following equations:

$$\left(\sigma_\varphi\right)_{\rho=a} = \frac{a^2 + b^2}{b^2 - a^2} q, \tag{5}$$

$$\left(\sigma_\varphi\right)_{\rho=b} = \frac{2a^2}{b^2 - a^2} q, \tag{6}$$

where $(\sigma_\varphi)_{\rho=a}$ and $(\sigma_\varphi)_{\rho=b}$ are the tensile stress on the inner wall and on the outer wall of the sleeve.

The friction between the specimen and the sleeve is ignored, and the compressive stress on the inner wall of the sleeve is equal to the confining pressure of the ready-mixed concrete sample supplied to the sleeve. According to the hoop stress waveform on the outer wall of the sleeve, the passive confining pressure is calculated by the following equation:

$$\sigma_3 = q = \frac{b^2 - a^2}{2a^2}\left(\sigma_\varphi\right)_{\rho=b}, \tag{7}$$

where σ_3 is the passive confining pressure applied to the specimen by the sleeve.

3. Results and Discussion

3.1. Analysis of Dynamic Compressive Strength. Figures 6–8 illustrate the measured dynamic compressive strength of ready-mixed concrete based on the experimental data in uniaxial load and passive confining pressure states. In order to better describe the influence of water content and storage period on dynamic compressive strength, an important characteristic parameter defined in the paper is the dynamic strength loss rate η, which can be calculated according to the following equation:

$$\eta = \frac{\sigma_m - \sigma_0}{\sigma_0}, \tag{8}$$

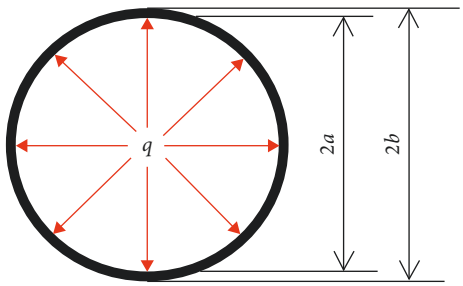

Figure 5: Force state diagram of steel sleeve subjected to passive confining pressure.

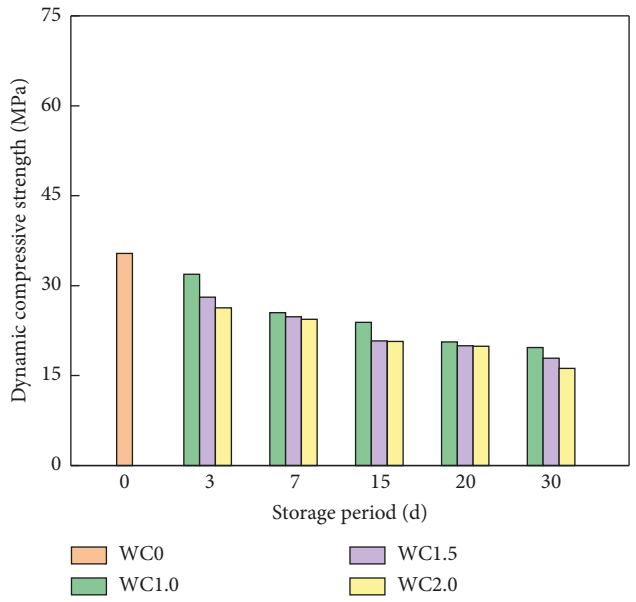

Figure 6: Dynamic compressive strength of ready-mixed concrete specimens with 0.6 MPa impact pressure in uniaxial load state.

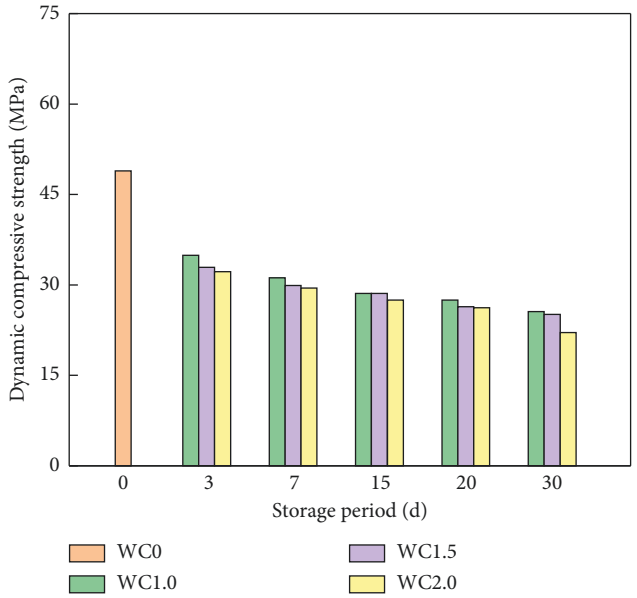

Figure 7: Dynamic compressive strength of ready-mixed concrete specimens with 0.9 MPa impact pressure in uniaxial load state.

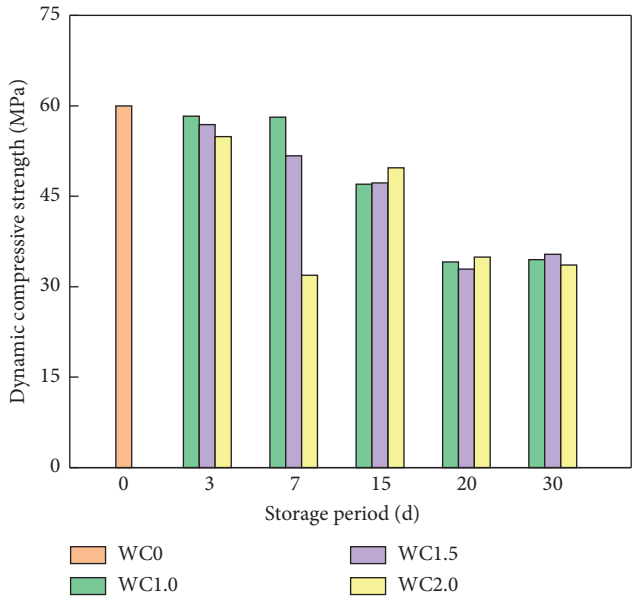

Figure 8: Dynamic compressive strength for ready-mixed concrete with 0.9 MPa impact pressure in passive confining pressure state.

where, σ_m is the dynamic compressive strength of ready-mixed concrete with different water contents and storage periods and σ_0 is the dynamic compressive strength of ready-mixed concrete without storage period and water content.

Figure 6 shows the effects of water content and storage period on dynamic compressive strength of ready-mixed concrete with 0.6 MPa impact pressure in uniaxial load state. It can be seen from Figure 6 that water content and storage period play an important role in dynamic compressive strength of ready-mixed concrete. At the same water content, the dynamic compressive strength of ready-mixed concrete decreases with the increase of storage period, which decreases rapidly with storage period from 0 d to 3 d and decreases slowly with storage period from 3 d to 30 d. It also indicates that the relationship of storage period and dynamic compressive strength shows an exponential trend. Under the condition of 1.0%, 1.5%, and 2.0% water content, dynamic compressive strength of ready-mixed concrete with 30 d storage period decreases by 44.35%, 49.44%, and 54.24% as compared to that of ready-mixed concrete without storage period. The mechanism behind this phenomenon can be explained as follows. As the storage period increases, the degree of hydration reaction inside the ready-mixed dry material is higher, and hydrated products such as C-S-H and AFt crystals are formed. These hydration products enclose the cement particles, which prevent or delay the continued hydration of cement inside concrete made of ready-mixed dry material. This ultimately leads to loose and low-density internal structural features of ready-mixed concrete. Meanwhile, these loose structures become the weak surface of the ready-mixed concrete, which increases the number of pores and enlarges the pore size, resulting in decreasing the dynamic compressive strength of ready-mixed concrete.

Figure 6 also shows that at the same storage period, the dynamic compressive strength of ready-mixed concrete decreases with increasing water content from 0% to 2.0%. Under the condition of 3 d, 7 d, 15 d, 20 d, and 30 d storage period, dynamic compressive strength of ready-mixed concrete with 2.0% water content decreases by 25.71%, 31.07%, 41.53%, 43.79%, and 54.24% as compared to that of ready-mixed concrete without water content. The above experimental results are similar to the previous study of static mechanics performed by Zhang and Ma [16]. The effects of water content on dynamic compressive strength might be due to the following reasons: (1) As the water content increases, the hydration reaction of the ready-mixed dry material consumes the more cement and the amount of cement inside ready-mixed concrete involved in hydration reaction is reduced, which results in decreasing the amount of hydration products and the compactness of the structure for ready-mixed concrete. (2) The amount of water added into ready-mixed concrete is constant in the process of concrete production, which is equivalent to indirectly increasing the ratio between water and cementitious materials and reducing the amount of cementitious materials inside ready-mixed concrete with increasing water content. It is more likely to increase the internal porosity after hardening for concrete. (3) That the addition of water is stirred during concrete making process destroys the structure of the formed hydrated product, which reduces the internal structure cementing ability of the ready-mixed concrete.

Figure 7 shows the variation of dynamic compressive strength of ready-mixed concrete specimens with 0.9 MPa impact pressure in uniaxial load state. From Figure 7, it can be seen that the dynamic compressive strength of ready-mixed concrete decreases with increasing water content and storage period, which is similar to the result of specimens with 0.6 MPa impact pressure in uniaxial load state. However, compared with Figure 6, Figure 7 shows that impact pressure has a significant influence on improving dynamic compressive strength for ready-mixed concrete specimens. In other words, at the same water content and storage period, the dynamic compressive strength of ready-mixed concrete in uniaxial load state increases as impact pressure increases. In both figures, under the condition of 0% water content and 0 d storage period, the dynamic compressive strength of specimens with 0.9 MPa impact pressure is 48.9 MPa, increasing by 38.14% as compared to that of specimens with 0.6 MPa impact pressure (35.4 MPa). As the water content increases from 1.0% to 2.0%, the dynamic compressive strength of specimens with 0.9 MPa impact pressure increases by 29.95%, 40.22%, and 36.42% as compared with that of specimens with 0.6 MPa impact pressure under the condition of 30 d storage period. Meanwhile, under the condition of 3 d, 7 d, 15 d, 20 d, and 30 d storage period, the dynamic compressive strength of ready-mixed concrete with 0.9 MPa impact pressure increases by 22.43%, 20.90%, 32.85%, 31.66%, and 36.42% as compared with that of ready-mixed concrete with 0.6 MPa impact pressure at the same water content (2.0%). This experimental result is in agreement with the previous research performed by Ping et al. [4], indicating that impact pressure can effectively strengthen the dynamic compressive strength of ready-mixed concrete.

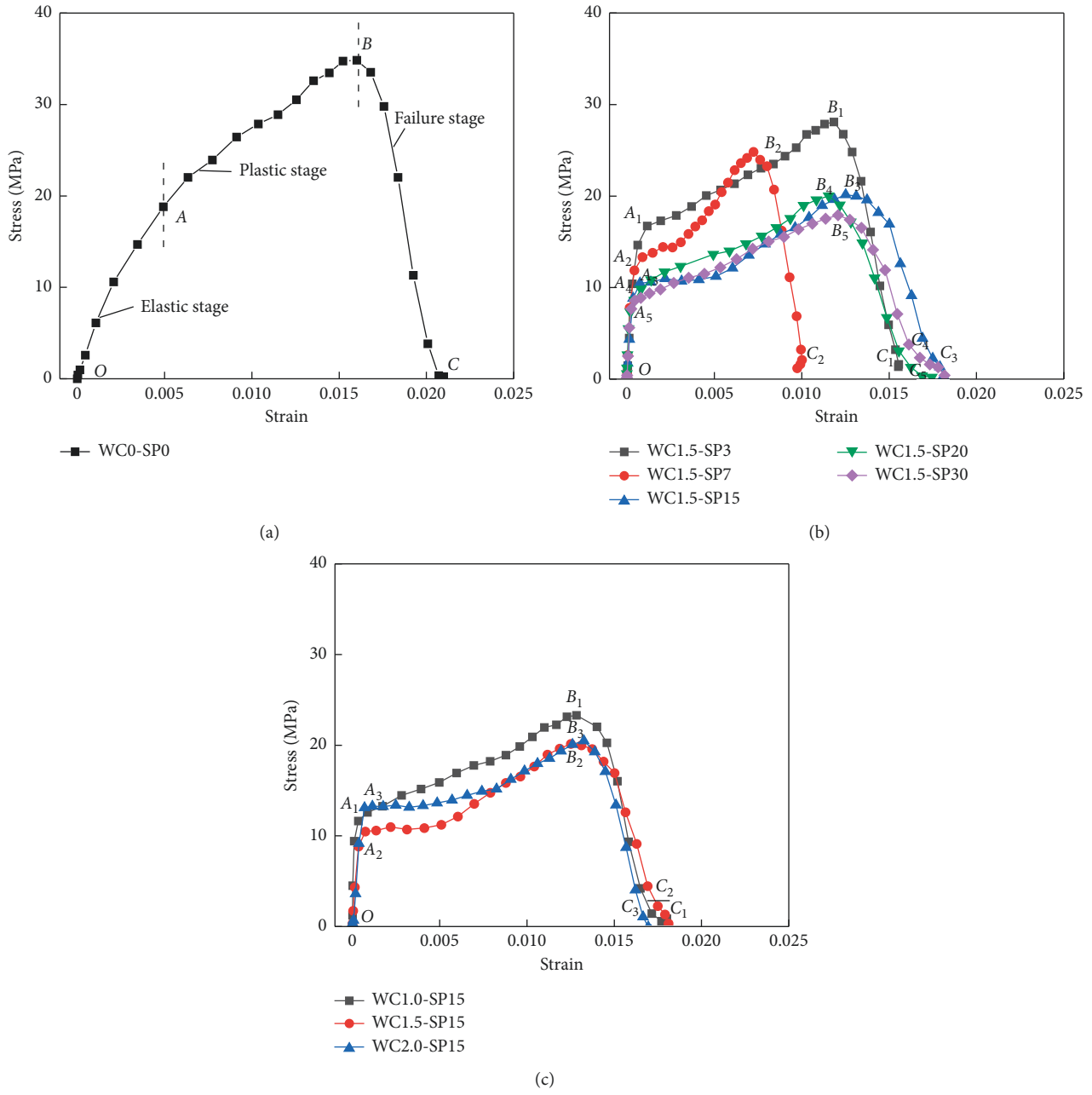

Figure 9: Dynamic stress-strain curves for ready-mixed concrete with 0.6 MPa impact pressure in uniaxial load state.

Figure 8 shows the effect of passive confining pressure on the dynamic compressive strength for ready-mixed concrete with 0.9 MPa impact pressure. A comparison of Figures 6 and 7 with Figure 8 shows that the passive confining pressure makes contribution to the enhancement of the dynamic compressive strength of ready-mixed concrete. At the same impact pressure (0.9 MPa), the dynamic compressive strength of ready-mixed concrete in passive confining pressure state is more than that of ready-mixed concrete in uniaxial load state; however, the degree of alteration is quite different. Under the condition of 0% water content and 0 d storage period, the dynamic compressive strength of specimens in passive confining pressure state is 60 MPa, increasing by 22.70% as compared with that of specimens in uniaxial load state (48.9 MPa). As the water content increases from 1.0% to 2.0%, the dynamic compressive strength of specimens in passive confining pressure state increases by 25.80%, 41.04%, and 52.04% as compared with that of specimens in uniaxial load state under the condition of 30 d storage period. Meanwhile, under the condition of 3 d, 7 d, 15 d, 20 d, and 30 d storage period, the dynamic compressive strength of ready-mixed concrete in passive confining pressure state increases by 70.50%, 8.14%, 80.73%, 33.21%, and 52.04% as compared with that of ready-mixed concrete in uniaxial load state at the same water content (2.0%), which shows that the dynamic compressive strength in passive confining pressure state is about 1.5 times as compared with that in uniaxial load state.

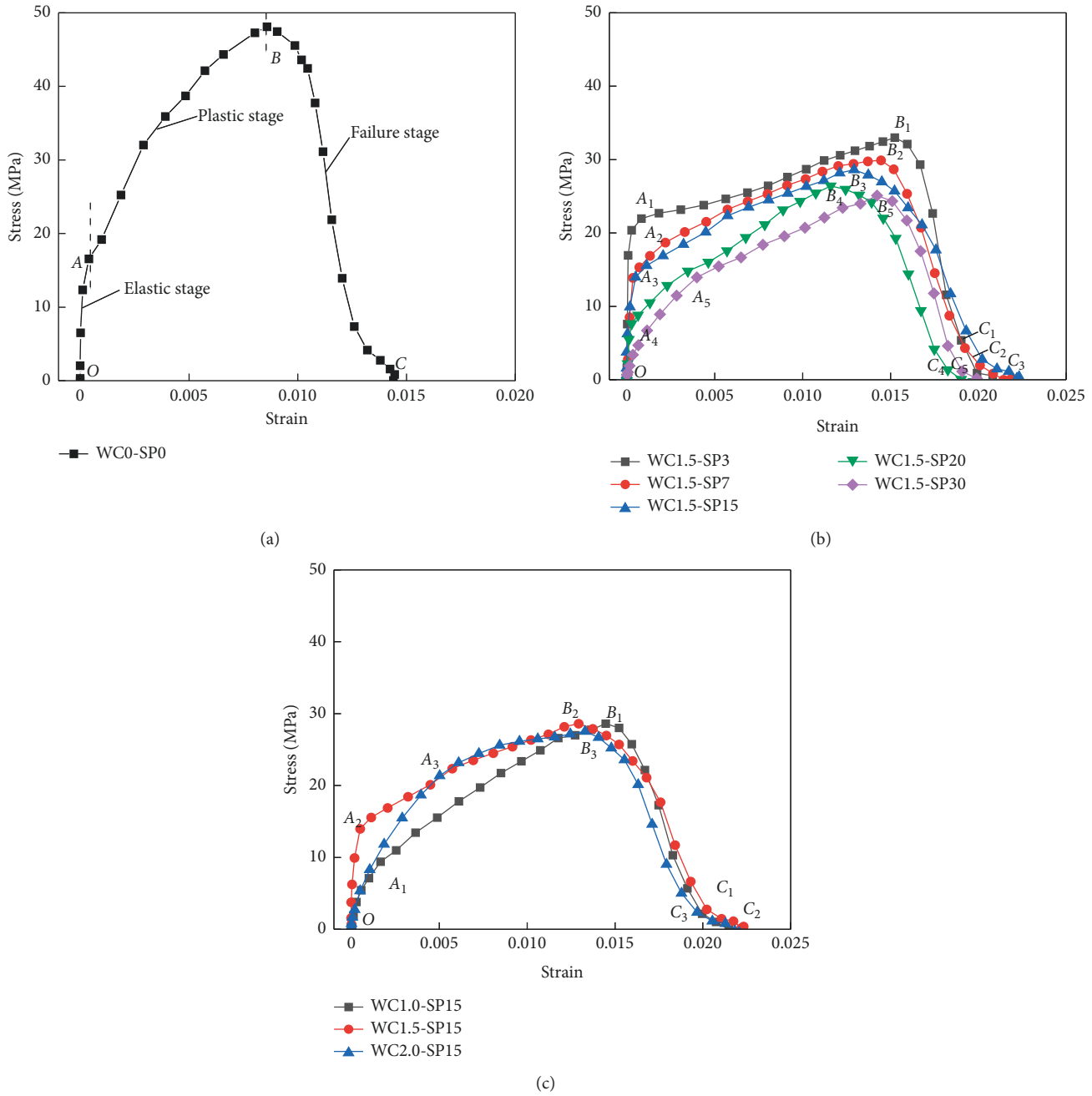

Figure 10: Dynamic stress-strain curves for ready-mixed concrete with 0.9 MPa impact pressure in uniaxial load state.

As can be seen from Figure 8, the variation of dynamic compressive strength for ready-mixed concrete specimens with different water contents and storage periods in passive confining pressure state is similar to that of ready-mixed concrete specimens in uniaxial load state, which generally shows a downward trend. However, dynamic compressive strength for ready-mixed concrete specimens with 2.0% water content and 7 d storage period decreases sharply, this phenomenon may be due to the following two reasons. On the one hand, there are many internal cracks, holes, and pores inside the ready-mixed concrete specimens caused by uneven vibration during the manufacturing process. On the other hand, when the impact occurs, the upper and lower surfaces of the specimens are not close to the rod. The above figures also show that the dynamic compressive strength decreases at a relatively slow rate within 15 d. As the storage period increases from 15 to 20 d, the dynamic compressive strength decreases rapidly, further increasing with storage period from 20 d to 30 d, which results in substantially constant for dynamic compressive strength. The dynamic compressive strength of ready-mixed concrete in passive confining pressure state is more than 30 MPa, meeting the static compressive strength standard value of C30 concrete.

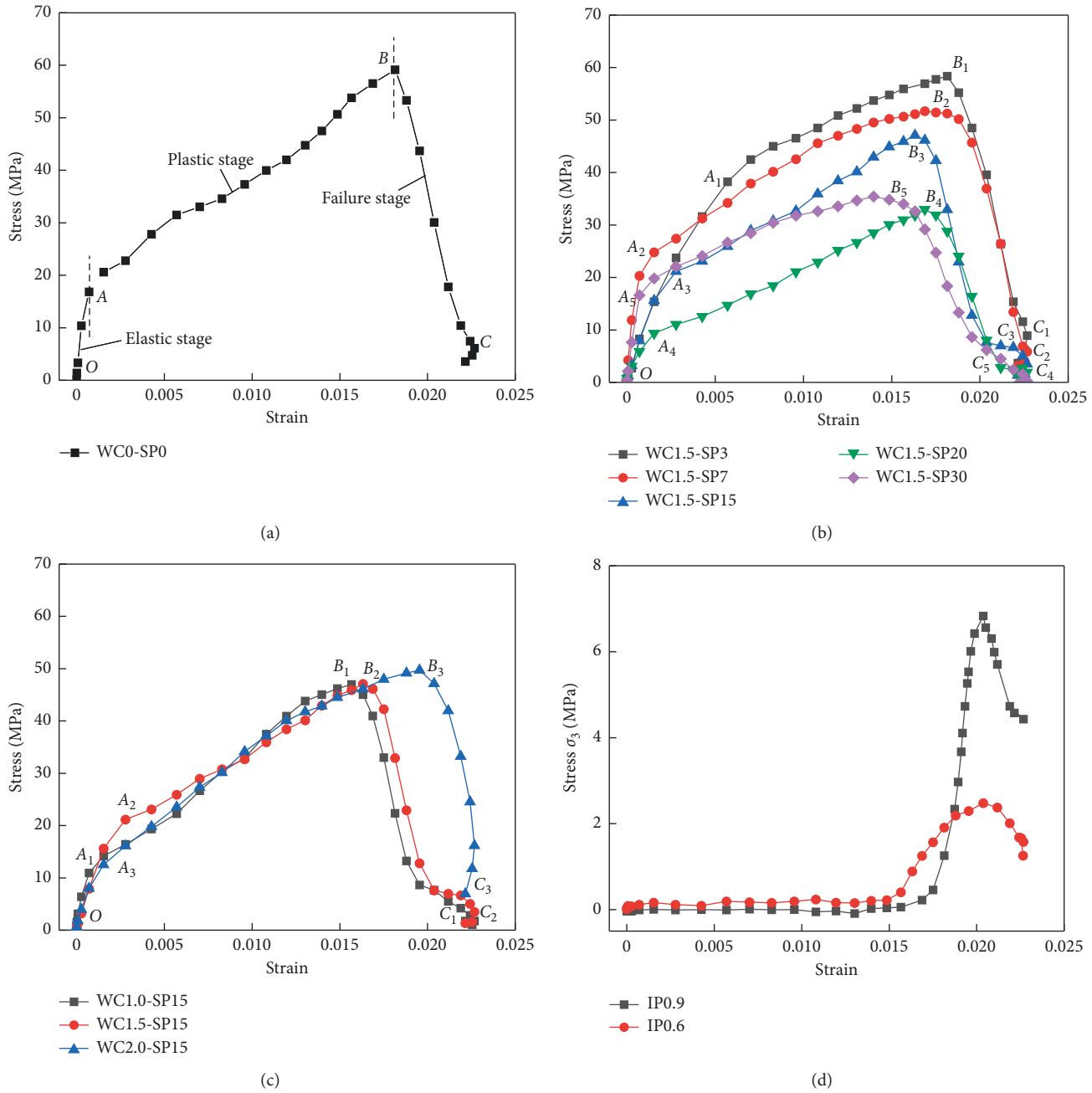

Figure 11: Dynamic stress-strain curves for ready-mixed concrete with 0.9 MPa impact pressure in passive confining pressure state.

3.2. Dynamic Stress-Strain Behavior. The typical dynamic stress-strain behaviors provide an understanding of the deformation and dynamic strength characteristics of ready-mixed concrete with different water contents, storage periods, and impact pressures, as presented in Figures 9–11. In these figures, Figures 9 and 10 present dynamic stress-strain curves for ready-mixed concrete in uniaxial load state, while Figure 11 shows dynamic stress-strain curves for ready-mixed concrete in passive confining pressure state. It can be seen from the figures that the stress increases with increasing strain before the stress reaches its peak and then decreases sharply. Based on SHPB test results, dynamic stress-strain curves for ready-mixed concrete in uniaxial load and passive confining pressure states, as shown in these figures, can be roughly divided into three stages: (1) linear elastic stage (OA), the stress of ready-mixed concrete linearly increases as the strain increases, which is mainly due to the microcracks inside the sample being not closed; (2) plastic yield stage (AB), the stress of ready-mixed concrete has a relative slower and fluctuating trend with the increase of the strain before the stress reaches its peak, which is mainly because of waveform oscillation at the incident loading stress wave head; and (3) failure stage (BC), the stress decreases sharply, whereas strain increases slightly, which shows that the bearing capacity decreases after the stress reaches its peak. However, from these figures, the dynamic stress-strain

curves with different water contents, storage periods, and impact pressures show the degree of alteration.

Figure 9 presents dynamic stress-strain curves for ready-mixed concrete with 0.6 MPa impact pressure in uniaxial load state. It can be observed from Figure 9 that the value of peak strain with 0.6 MPa impact pressure shows a trend of fluctuation with increasing storage periods and water contents, while the peak stress of ready-mixed concrete decreases as storage periods and water contents increase.

Figure 10 shows dynamic stress-strain curves for ready-mixed concrete with 0.9 MPa impact pressure in uniaxial load state. As shown in Figures 10(a) and 10(b), the value of peak strain with 1.5% water content and varying storage periods is 0.0152, 0.0145, 0.0129, 0.0116, and 0.0142, which increases generally as compared with that of peak strain without storage period and water content (0.0086). It can be observed from Figure 10(c) that the value of peak strain with 15 d storage period and varying water content is 0.0144, 0.0129, and 0.0133, which is greater than that of peak strain without storage period and water content. Therefore, under the condition of 0.9 MPa uniaxial impact pressure, storage period and water content can increase the peak strain of ready-mixed concrete, but the reduction ratio of peak stress varies with storage periods and water contents, which is likely due to the structural damage of ready-mixed concrete. The experimental result is similar to ready-mixed concrete with 0.6 MPa impact pressure. In addition, a comparison of Figure 9 with Figure 10 can find that impact pressure has significant influence on dynamic stress-strain relationships, which can clearly show that the peak stress and the peak strain increase with increasing impact pressure from 0.6 MPa to 0.9 MPa, and initial slope related to the initial modulus increases greatly.

Additionally, a comparison of Figures 9 and 10 with Figure 11 shows that the dynamic stress-strain curves for ready-mixed concrete with 0.9 MPa impact pressure in passive confining pressure state. It is clear that the peak strain of ready-mixed concrete gradually decreases with increasing storage periods, which presents a more stable trend as compared with that of ready-mixed concrete in uniaxial load state, while the influence of water content corresponding to the peak strain is consistent with that of ready-mixed concrete in uniaxial load state. Meanwhile, the peak stress and the peak strain increase with the application of confining pressure, which is due to changing the force state of sample, inhibiting the expansion of the internal crack, and improving the resistance of the sample to damage. Through the analysis of experimental data, it is found that compared with the water content and storage period, the impact pressure has a greater influence on the confining pressure. Therefore, this paper analyzes that at the same water content and storage period, the confining pressure with different impact pressures is collected through confining pressure waves. It can be observed from Figure 11 that confining pressure σ_3 increases slowly with the strain from 0 to 0.015; the confining pressure increases sharply, whereas there is a slight increase in the strain from 0.015 to 0.021; the confining pressure decreases quickly with increasing the strain after the confining pressure reaches its peak. In addition, the peak stress of confining pressure with 0.9 MPa impact pressure is much larger than that with 0.6 MPa impact pressure, which is consistent with the experimental result of the previous study by Li et al. [43].

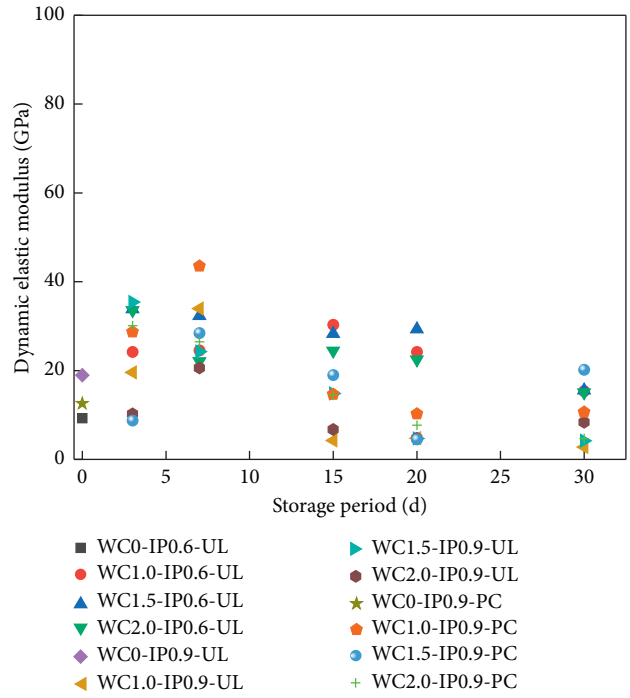

Figure 12: Dynamic elastic modulus of ready-mixed concrete. The coordinates of the dynamic elastic modulus axis is modified to 0–50 GPa and divided into five parts in units of 10 GPa..

3.3. Dynamic Elastic Modulus. Dynamic elastic modulus used to evaluate the behavior of deformation in this research is defined as the slope of straight line formed by connecting 40% of the peak stress on the stress-strain curve to the origin [44, 45], which is calculated through the following equation:

$$E = \frac{\Delta\sigma}{\Delta\varepsilon} = \frac{\sigma_{0.4} - \sigma_0}{\varepsilon_{0.4} - \varepsilon_0}, \tag{9}$$

where $\sigma_{0.4}$ and σ_0 represent the peak stress of 40% and the origin corresponding to the strain $\varepsilon_{0.4}$ and ε_0 from Figures 9–11, respectively.

The calculated results, as shown in Figure 12, show that the dynamic elastic modulus E is different due to the difference of intercepted line segment on the curve. Figure 12 shows that there is a certain fluctuation in the dynamic elastic modulus; however, it can be seen from the above figures that the dynamic elastic modulus decreases with the increase of storage period in general. The above result is similar to the conclusions drawn by Yang [46]. The main reason maybe that the hydrated cement of ready-mixed dry material reduces the hydration product of ready-mixed concrete. Dynamic elastic modulus, with increasing storage periods from 0 d to 15 d, decreases sharply, further increasing the storage period from 15 d to 30 d, and changes relatively slowly. As impact pressure increases, dynamic

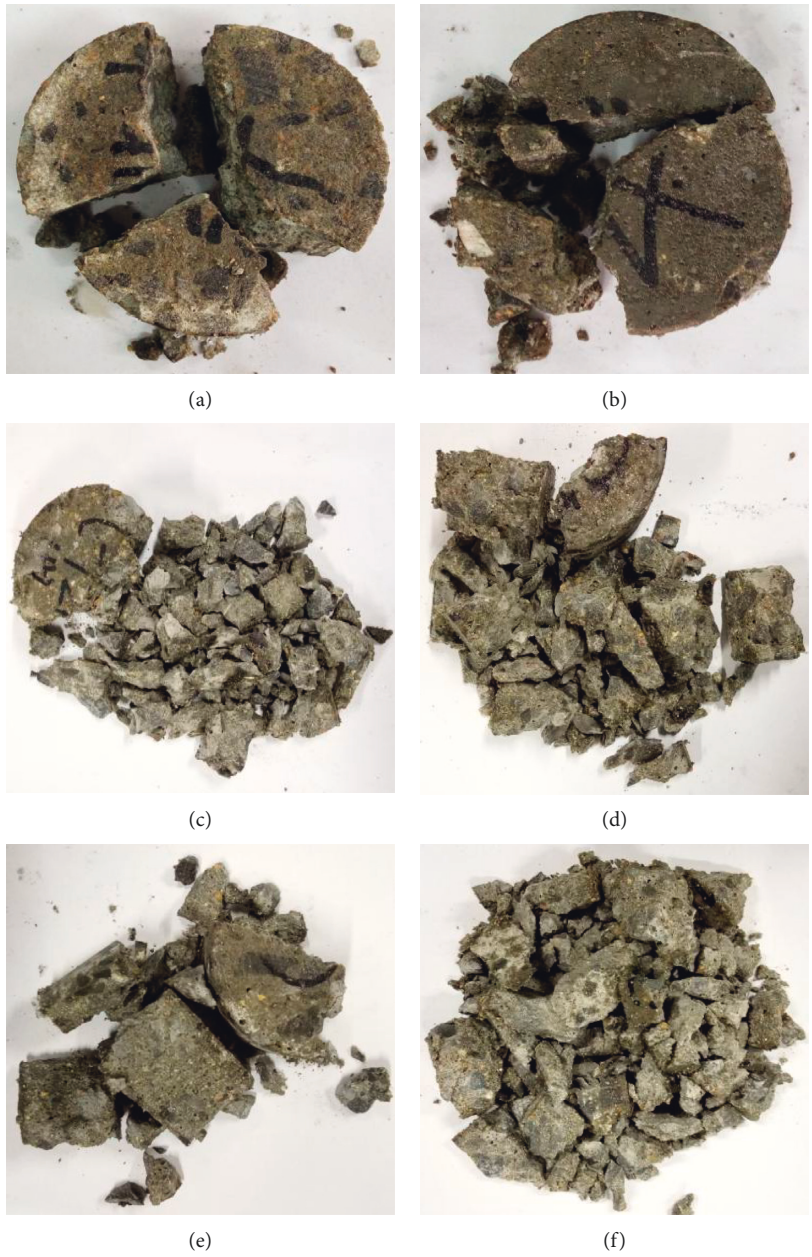

Figure 13: Failure mode of ready-mixed concrete in uniaxial load state. (a) WC0-SP0. (b) WC2.0-SP3. (c) WC2.0-SP7. (d) WC2.0-SP15. (e) WC2.0-SP20. (f) WC2.0-SP30.

elastic modulus of ready-mixed concrete without water content and storage period ranges from 9.26 GPa to 18.97 GPa in uniaxial load state. Dynamic elastic modulus in passive confining pressure state is more than that in uniaxial load state in general, which shows that passive confining pressure can improve the deformation of ready-mixed concrete. However, partial dynamic elastic modulus in passive confining pressure state is less than that in uniaxial load state, which maybe that the probe is unstable in the early stage of the test and the straight line segment of stress-strain curve in uniaxial load state has a large discrete type. In summary, for ready-mixed concrete in uniaxial load and passive confining pressure states, E is a parameter influenced by the interaction of water content, storage period, and impact pressure. Meanwhile, passive confining pressure has a greater impact on dynamic elastic modulus.

3.4. Failure Modes of Specimens. At the same impact pressure (0.9 MPa), failure modes of ready-mixed concrete specimens studied by the dynamic compressive test in uniaxial load and passive confining pressure states are shown in Figures 13 and 14, respectively. It is clearly noticed that the degree of damage for ready-mixed concrete specimens increases with the increase of the storage period and water content. More specifically, with the storage period and water content increasing, the number of fragments increases and the grain size of fragments becomes smaller. When the storage period

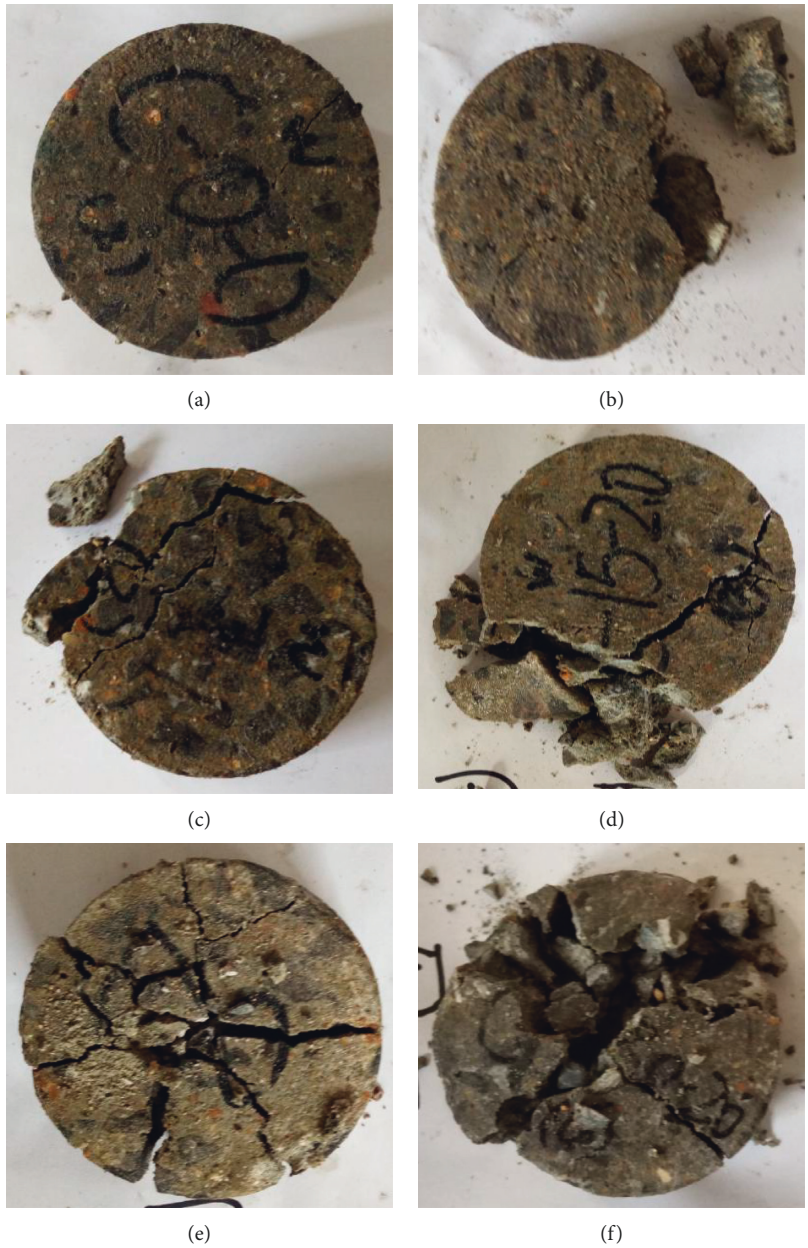

Figure 14: Failure modes of ready-mixed concrete in passive confining pressure state. (a) WC0-SP0. (b) WC2.0-SP3. (c) WC2.0-SP7. (d) WC2.0-SP15. (e) WC2.0-SP20. (f) WC2.0-SP30.

is 30 d and the water content is 2.0%, the damage of specimens in uniaxial load and passive confining pressure states is most serious. As clear in Figure 13, under the condition of uniaxial load state, the failure of specimens expands from the edge to the center, which is more uniform and thorough with increasing water content and storage period. Meanwhile, a phenomenon like above happens to the ready-mixed concrete specimens in passive confining pressure state (Figure 13). When the storage period and water content of ready-mixed dry material are small, the ready-mixed concrete specimen exhibits splitting damage, while those of ready-mixed dry material are large, the specimen exhibits crushing damage, indicating that the strength of the ready-mixed concrete decreases and the brittleness increases. The result is similar to the conclusions drawn by Wu et al. [47].

However, the number of fragments in uniaxial load state is more than that in passive confining pressure and the grain size of fragments in uniaxial load state is generally smaller than that in passive confining pressure, which indicates that the effect of passive confining pressure can reduce the damage degree of ready-mixed concrete. Due to the sleeve constraint, the stress state of specimen is changed from a one-dimensional stress state to a three-direction stress state, which inhibits the brittle fracture of the specimen caused by the evolution of the damage, further improving the ductility and resistance to damage of ready-mixed concrete specimen [48].

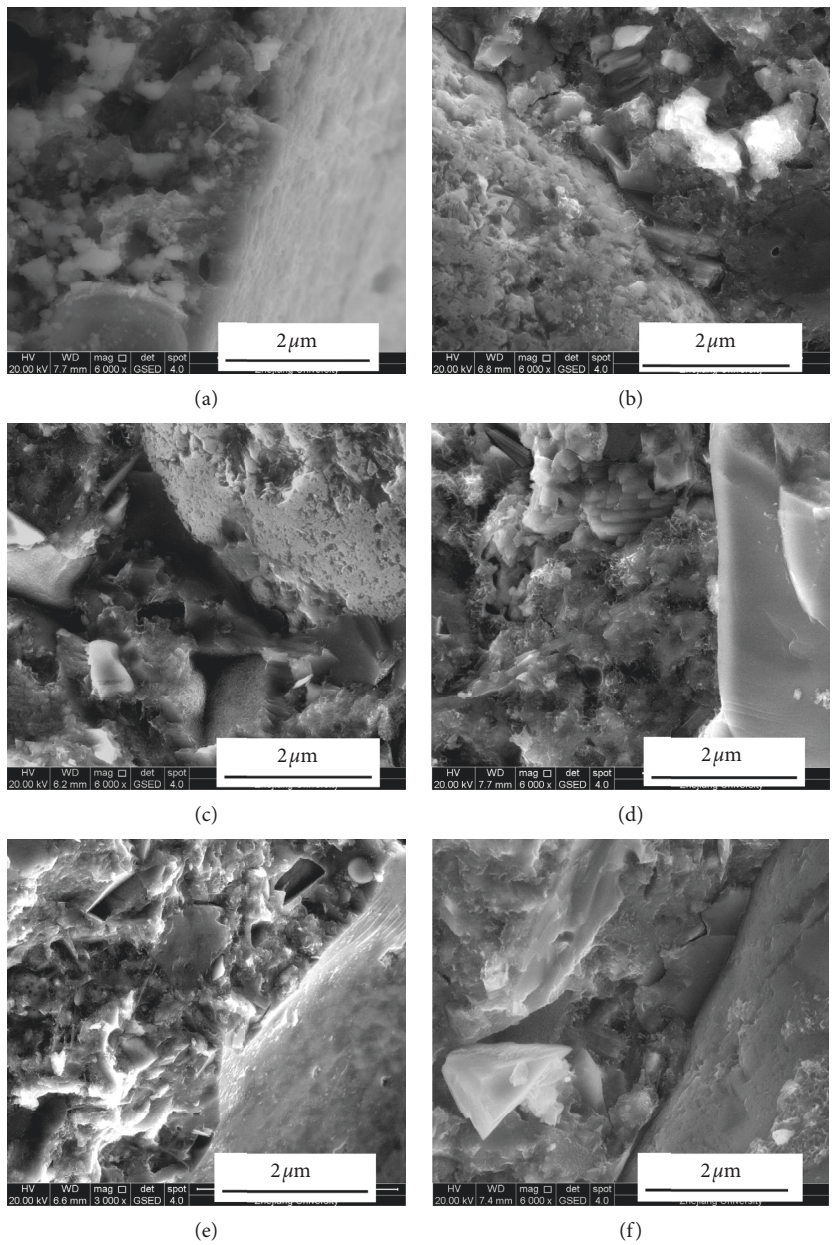

Figure 15: SEM images of ready-mixed concrete with different water contents and storage periods. (a) WC1.5-SP3. (b) WC1.5-SP7. (c) WC1.5-SP15. (d) WC1.5-SP30. (e) WC2.0-SP30. (f) WC1.0-SP30.

4. Microscopic Mechanism Analysis of Ready-Mixed Concrete

In order to analyze the microscopic mechanism of the ready-mixed concrete with different water contents and storage periods, the microscopic test based on the scanning electron microscope (SEM) are conducted. Representative SEM images, as shown in Figure 15, illustrate that the hydration products of ready-mixed concrete with different water contents and storage periods have obvious differences, which plays a fundamental role in internal structure.

It can be clearly seen from Figures 15(a)–15(d) that under the condition of 1.5% water content, microstructure of ready-mixed concrete changes with storage periods from 3 d to 30 d. There are less fine threads on the matrix surface of ready-mixed concrete when the storage period is less than 3 d, which corresponds to ettringite products formed from the hydration reactions of cement. Meanwhile, the interfacial transition zone of the ready-mixed concrete is low density and loose structure, and there are more cement particles with lower hydration degree, which indicates that shorter storage period has little effect on the hydration reaction of the ready-mixed concrete. As storage period increases, the interfacial transition zone mainly contains a large amount of loose flaky calcium hydroxide, which results in the interface structure being poor. Internal structure of ready-mixed concrete with 30 d storage period exists some shrinkage cracks found in the interfacial transition zone.

Figures 15(d)–15(f) show SEM images of ready-mixed concrete with 30 d storage periods and varying water contents. It can be seen from Figures 15(d)–15(f) that the hydration reaction of the ready-mixed concrete with 1.0% water content is slow and the hydration products are less. As water content increases 2.0%, the C-S-H gel of ready-mixed dry material continues to increase and the cement particles are substantially free of angular edges, forming a staggered ettringite filled between the cement particles, which leads to extending interface transition zone of ready-mixed concrete and forming loose microstructure. Ready-mixed concrete made of ready-mixed dry material with water is stirred, which destroys the structure of the original hydration product that has lost its cementation ability. Meanwhile, the unhydrated cement particles are difficult to enter into these loose microscopic hydration products [49]. Therefore, the above reasons lead to reducing dynamic compressive strength of ready-mixed concrete. This explains the effect of water content and storage period on the macroscopic dynamic mechanical properties of ready-mixed concrete from a microscopic point of view.

5. Conclusions

This paper investigates the effects of water content, storage period, and impact pressure on the dynamic mechanical properties of ready-mixed concrete based on the SHPB test. The dynamic strength, the dynamic stress-strain curve, failure modes, and microstructure of ready-mixed concrete are analyzed. The following conclusions can be drawn from the present study:

(1) The dynamic compressive strength of ready-mixed concrete decreases with increasing water content and storage period in uniaxial load and passive confining pressure states but increases with the increase of impact pressure. Meanwhile, at the same water content, storage period, and impact pressure, the dynamic compressive strength of ready-mixed concrete in passive confining pressure state is about 1.5 times as compared with that in uniaxial load state.

(2) Dynamic stress-strain curves for ready-mixed concrete in uniaxial load and passive confining pressure states can be divided into linear elastic stage, plastic yield stage, and failure stage. Peak strain and dynamic elastic modulus of ready-mixed concrete in the passive confining pressure states are more than that in uniaxial load state.

(3) When the storage period and water content are small, the ready-mixed concrete specimen exhibits splitting damage, whereas when they are large, it exhibits crushing damage. SEM analysis revealed that interface transition zone of ready-mixed concrete gradually expands as the storage period and water content increase. Under the condition of 30 d storage period and 2.0% water content, the damage degree of ready-mixed concrete is most serious in the experiment. Meanwhile, the effect of passive confining pressure can reduce the damage degree of ready-mixed concrete.

Data Availability

The datasets generated and analyzed during the current study are available from the corresponding author upon reasonable request.

Conflicts of Interest

The authors confirm that this article has no conflicts of interest regarding the publication of this paper.

Acknowledgments

This research was funded by the Natural Science Research Project of Colleges and Universities in Anhui Province (no. KJ2015A135). The authors are sincerely grateful to the Engineering Research Center of Underground Mine Construction, Ministry of Education, Anhui University of Science and Technology, for providing the experiment conditions and Zhejiang University for supporting the SEM test.

References

[1] J. Guo, J. Cai, Q. Chen, X. Liu, Y. Wang, and Z. Zuo, "Dynamic behaviour and energy dissipation of reinforced recycled aggregate concrete beams under impact," *Construction and Building Materials*, vol. 214, pp. 143–157, 2019.

[2] M. Koushkbaghi, P. Alipour, B. Tahmouresi, E. Mohseni, A. Saradar, and P. K. Sarker, "Influence of different monomer ratios and recycled concrete aggregate on mechanical properties and durability of geopolymer concretes," *Construction and Building Materials*, vol. 205, no. 2, pp. 519–528, 2019.

[3] C. L. Xin, Z. Z. Wang, J. M. Zhou, and B. Gao, "Shaking table tests on seismic behavior of polypropylene fiber reinforced concrete tunnel lining," *Tunnelling and Underground Space Technology*, vol. 88, pp. 1–15, 2019.

[4] Q. Ping, Q. Y. Ma, X. Y. Lu, and W. Yuan, "Impact compression test of rock material under passive confining pressure conditions," *Chinese Journal of Vibration and Shock*, vol. 33, no. 2, pp. 55–59, 2014.

[5] X. B. Li, J. Zhou, S. F. Wang, and B. Liu, "Review and practice of deep mining for solid mineral resources," *Chinese Journal of Nonferrous Metals*, vol. 27, no. 6, pp. 1236–1262, 2017.

[6] S. Li, B. Xie, S. Hu et al., "Removal of dust produced in the roadway of coal mine using a mining dust filtration system," *Advanced Powder Technology*, vol. 30, no. 5, pp. 911–919, 2019.

[7] X. Tan, W. Chen, H. Liu et al., "A combined supporting system based on foamed concrete and U-shaped steel for underground coal mine roadways undergoing large deformations," *Tunnelling and Underground Space Technology*, vol. 68, pp. 196–210, 2017.

[8] D. Xuan, C. S. Poon, and W. Zheng, "Management and sustainable utilization of processing wastes from ready-mixed concrete plants in construction: a review," *Resources, Conservation and Recycling*, vol. 136, pp. 238–247, 2018.

[9] Z. Liu, Y. Zhang, and M. Li, "Integrated scheduling of ready-mixed concrete production and delivery," *Automation in Construction*, vol. 48, pp. 31–43, 2014.

[10] J. S. Zhang, *Research on Microstructure and Mechanical Properties of Ready-Mixed Concrete and Application in Mine*, Anhui University of Science and Technology, Huainan, China, 2014.

[11] GB/T 14902-2012, *National Standardization Administration of the People's Republic of China, National Standard of the People's Republic of China: Ready-Mixed Concrete (GB/T 14902-2012)*, China Standard Press, Beijing, China, 2012.

[12] A. M. Alhozaimy, "Effect of retempering on the compressive strength of ready-mixed concrete in hot-dry environments," *Cement and Concrete Composites*, vol. 29, no. 2, pp. 124–127, 2007.

[13] N. N. Gebremichael, S. M. Motahari Karein, M. Karakouzian, and K. Jadidi, "Investigation of setting time and compressive strength of ready-mixed concrete blended with returned fresh concrete," *Construction and Building Materials*, vol. 197, pp. 428–435, 2019.

[14] Y. Y. Zhang and Q. Y. Ma, "Effect of expansion agent and water content on microstructure of ready-mixed shrinkage-compensating concrete," *China Sciencepaper*, vol. 10, no. 13, pp. 1535–1538, 2015.

[15] H. M. Basar and N. Deveci Aksoy, "The effect of waste foundry sand (WFS) as partial replacement of sand on the mechanical, leaching and micro-structural characteristics of ready-mixed concrete," *Construction and Building Materials*, vol. 35, pp. 508–515, 2012.

[16] J. S. Zhang and Q. Y. Ma, "Cubic compressive test and microstructure of ready-mixed materials with different water contents," *Bulletin of the Chinese Ceramic Society*, vol. 32, no. 11, pp. 2331–2336, 2013.

[17] M. Li, H. Hao, Y. Shi, and Y. Hao, "Specimen shape and size effects on the concrete compressive strength under static and dynamic tests," *Construction and Building Materials*, vol. 161, pp. 84–93, 2018.

[18] L. Jin, W. Yu, X. Du, S. Zhang, and D. Li, "Meso-scale modelling of the size effect on dynamic compressive failure of concrete under different strain rates," *International Journal of Impact Engineering*, vol. 125, pp. 1–12, 2019.

[19] Y. B. Guo, G. F. Gao, L. Jing, and V. P. W. Shim, "Response of high-strength concrete to dynamic compressive loading," *International Journal of Impact Engineering*, vol. 108, pp. 114–135, 2017.

[20] X.-B. Li, S.-M. Wang, L. Weng, L.-Q. Huang, T. Zhou, and J. Zhou, "Damage constitutive model of different age concretes under impact load," *Journal of Central South University*, vol. 22, no. 2, pp. 693–700, 2015.

[21] Y. D. Jiang, Y. X. Zhao, Y. Q. Song, W. G. Liu, and D. J. Zhu, "Analysis of blasting tremor impact on roadway stability in coal mining," *Chinese Journal of Rock Mechanics and Engineering*, vol. 24, no. 17, pp. 3131–3136, 2005.

[22] L. Yuan, "Exploit coal and gas simultaneously lead scientific coal exploration," *Chinese Energy and Energy Conservation*, vol. 4, pp. 1–4, 2011.

[23] Q. Ma, D. Ma, and Z. Yao, "Influence of freeze-thaw cycles on dynamic compressive strength and energy distribution of soft rock specimen," *Cold Regions Science and Technology*, vol. 153, pp. 10–17, 2018.

[24] P. Yuan and Y. Xu, "Zonal disintegration mechanism of deep rock masses under coupled high axial geostress and blasting load," *Shock and Vibration*, vol. 2018, Article ID 4957917, 11 pages, 2018.

[25] C. J. Jiao, X. B. Li, C. M. Cheng, and C. B. Li, "Dynamic damage constitutive relation of high strength concrete based on fractal theory," *Chinese Explosion and Shock Waves*, vol. 38, no. 4, pp. 925–930, 2018.

[26] K.-M. Kim, S. Lee, and J.-Y. Cho, "Effect of maximum coarse aggregate size on dynamic compressive strength of high-strength concrete," *International Journal of Impact Engineering*, vol. 125, pp. 107–116, 2019.

[27] L. Ma, Z. Li, J. Liu, L. Duan, and J. Wu, "Mechanical properties of coral concrete subjected to uniaxial dynamic compression," *Construction and Building Materials*, vol. 199, pp. 244–255, 2019.

[28] N. Li, G. C. Long, Q. Fu et al., "Dynamic mechanical characteristics of filling layer self-compacting concrete under impact loading," *Archives of Civil and Mechanical Engineering*, vol. 19, no. 3, pp. 851–861, 2019.

[29] JGJ 63-2006, *Ministry of Construction of the People's Republic of China, Standards of Water for Concrete (JGJ 63-2006)*, China Building Industry Press, Beijing, China, 2006.

[30] GB/T 50081-2002, *Ministry of Construction of the People's Republic of China, Standard for Test Method of Mechanical Properties on Ordinary Concrete (GB/T 50081-2002)*, China Building Industry Press, Beijing, China, 2002.

[31] ISRM, *Te Complete ISRM Suggested Methods for Rock Characterization, Testing and Monitoring*, R. Ulusay and J. Hudson, Eds., pp. 1974–2006, International Society for Rock Mechanics, Salzburg, Austria, 2007.

[32] Y. B. Wang, "Rock dynamic fracture characteristics based on NSCB impact method," *Shock and Vibration*, vol. 2018, Article ID 3105384, 13 pages, 2018.

[33] S. M. Wang, Y. S. Liu, J. Zhou, Q. H. Wu, S. Y. Ma, and Z. H. Zhou, "Dynamic compressive characteristics of sandstone under confining pressure and radial gradient stress with the SHPB test," *Advances in Civil Engineering*, vol. 2018, Article ID 1387390, 8 pages, 2018.

[34] S. M. Wang, L. J. Dong, and J. Zhou, "Influence of early age on the wave velocity and dynamic compressive strength of concrete based on split Hopkinson pressure bar tests," *Shock and Vibration*, vol. 2018, Article ID 8206287, 8 pages, 2018.

[35] L. Li, R. Zhang, L. Jin, X. Du, J. Wu, and W. Duan, "Experimental study on dynamic compressive behavior of steel fiber reinforced concrete at elevated temperatures," *Construction and Building Materials*, vol. 210, pp. 673–684, 2019.

[36] F. Yang, H. Ma, L. Jing, L. Zhao, and Z. Wang, "Dynamic compressive and splitting tensile tests on mortar using split Hopkinson pressure bar technique," *Latin American Journal of Solids and Structures*, vol. 12, no. 4, pp. 730–746, 2015.

[37] D.-d. Ma, Q.-y. Ma, Z.-m. Yao, P. Yuan, and R.-r. Zhang, "Dynamic mechanical properties and failure mode of artificial frozen silty clay subject to one-dimensional coupled static and dynamic loads," *Advances in Civil Engineering*, vol. 2019, Article ID 4160804, 9 pages, 2019.

[38] W. M. Li, J. Y. Xu, L. J. Shen, and Q. Li, "Study on 100-mm-diameter SHPB techniques of dynamic stress equilibrium and nearly constant strain rate loading," *Journal of Vibration and Shock*, vol. 27, no. 2, pp. 129–132, 2008.

[39] D. Ma, Q. Ma, and P. Yuan, "SHPB tests and dynamic constitutive model of artificial frozen sandy clay under confining pressure and temperature state," *Cold Regions Science and Technology*, vol. 136, pp. 37–43, 2017.

[40] Q. Y. Ma and C. H. Gao, "Effect of basalt fiber on the dynamic mechanical properties of cement-soil in SHPB test," *Journal of Materials in Civil Engineering*, vol. 30, no. 8, Article ID 04018185, 2018.

[41] L. Song and S. S. Hu, "Two-wave and three-wave method in SHPB data processing," *Chinese Explosion Shock Waves*, vol. 25, no. 4, pp. 368–373, 2005.

[42] J. L. Wu, *Elasticity*, Higher Education Press, Beijing, China, 2001.

[43] X. L. Li, D. S. Liu, M. D. Feng, S. G. Li, and Z. G. Yan, "Impact dynamic mechanical properties of concrete materials under

passive confining pressure of steel sleeves," *Chinese Explosion and Shock Waves*, vol. 29, no. 5, pp. 463–467, 2009.

[44] H. L. Dong, Y. K. Peng, K. J. Luo, D. C. Xue, W. P. Song, and Y. G. Ge, "Study on the rate sensitivity of high performance recycled concrete substituted by coarse aggregate," *Chinese Journal of Experimental Mechanics*, vol. 34, no. 2, pp. 249–257, 2019.

[45] K. J. Luo, *Dynamic Mechanical Properties and Strain Rate Effects of High Performance Recycled Concrete*, China University of Mining and Technology, Beijing, China, 2018.

[46] Y. L. Yang, *Experimental Study on Expansion Deformation and Crack Resistance of Ready-Mixed Shrinkage Concrete*, Anhui University of Science and Technology, Huainan, China, 2018.

[47] S. Wu, J. H. Zhao, N. Li, Y. Li, and Q. Zhu, "Study on dynamic mechanical properties of concrete in passive confining pressure state," *Chinese Journal of Applied Mechanics*, vol. 32, no. 6, pp. 992–998+1103, 2015.

[48] Q. Y. Ma, J. S. Zhang, W. F. Chen, and W. Yuan, "Study on the SHPB test and impact compression characteristics of artificial frozen soil under confining pressure," *Chinese Rock and Soil Mechanics*, vol. 35, no. 3, pp. 637–640, 2014.

[49] X.-L. Duan and J.-S. Zhang, "Mechanical properties, failure mode, and microstructure of soil-cement modified with fly ash and polypropylene fiber," *Advances in Materials Science and Engineering*, vol. 2019, Article ID 9561794, 13 pages, 2019.